Available online at www.sciencedirect.com

ScienceDirect

Ceramics International 40 (2014) 1797–1806

CERAMICS INTERNATIONAL

www.elsevier.com/locate/ceramint

Effect of milling on dielectric and microwave absorption properties of SiC based composites

Abhishek Kumar[a,*], Vijaya Agarwala[b], Dharmendra Singh[c]

[a]Applied Mechanics Department, Motilal Nehru National Institute of Technology Allahabad, Allahabad 211004, India
[b]Metallurgical & Materials Engineering Department, Indian Institute of Technology Roorkee, Roorkee 247667, India
[c]Electronics & Communication Engineering Department, Indian Institute of Technology Roorkee, Roorkee 247667, India

Received 13 June 2013; accepted 16 July 2013
Available online 24 July 2013

Abstract

The electromagnetic and microwave absorption properties of SiC-epoxy composites with the variation in particle size of SiC and dispersion of different metals in SiC have been studied. The micronsized SiC powder was reduced to nanosized SiC powder using high energy planetary ball mill. The results show the significant influence of particle size on the electromagnetic and microwave absorption properties. With the reduction in particle size, complex permittivity and microwave absorption of the epoxy composites have increased to a good extent. For further improvement in microwave absorption, different metal particles were dispersed in the SiC powder and as a result the microwave absorption properties were improved significantly. The values of RL for as-received SiC are improved from −16.23 dB at 10.888 GHz to −37.08 dB at 10.888 GHz with Cr-metal powder dispersion and −43.35 dB at 10.300 GHz with Mn-metal powder dispersion in SiC with 10 h milling. The corresponding 10 dB absorption bandwidth increased from 1.932 GHz to 3.024 GHz for Cr and Mn-metal powder dispersion. This study suggests that the reduction in particle size and metal dispersion in the SiC matrix are effective means to improve microwave absorption.
© 2013 Elsevier Ltd and Techna Group S.r.l. All rights reserved.

Keywords: SiC; Microwave absorption; Particle size; Metal dispersion

1. Introduction

In recent years, the problems of electromagnetic interference (EMI) due to the massive use of electromagnetic (EM) waves at higher frequencies in majority of electronic systems, satellite communication and military aircraft, have resulted into the development of new and much effective EM wave absorbers. These EMI problems may cause interruption in the electronic system and therefore, will reduce system performance. To avoid such problems, EM wave absorbers with a capability of absorbing undesired EM signals are required. Recent requirements for an EM absorber have resulted in the development of the materials that can efficiently absorb EM waves with reasonably good physical performance at lower cost [1–4]. The absorption of EM energy in a microwave absorbing material can be either due to ohmic losses or due to hysteresis losses. Dielectric materials like ceramics, conducting polymers and carbon are representative of absorbers based on the ohmic losses. Magnetic materials like ferrites are the absorbers based on the hysteresis loss [1,5,6]. The microwave absorbing characteristics of materials depend on their relative complex permittivity and complex permeability. By altering these dielectric properties, the improved absorption of the electromagnetic energy could be achieved. Silicon carbide (SiC) is an important carbide, studied as a structural ceramic for a long time and has attractive properties, such as high strength and hardness, good oxidation resistance, high thermal stability and creep resistance, that favors it for many structural applications [7,8]. Among other properties, SiC is a semiconductor with wide band gap, high electron saturation velocity, and high thermal conductivity, which makes it more attractive for high temperature applications [5,6,9–11]. On the other hand, SiC is used as EM absorbing material because of its good dielectric properties at microwave frequency [9–15]. Much work have been reported about the synthesis and dielectric constant measurement of SiC at micro- and nanometer sized particles. However, a very few studies are reported to see the effect of

*Corresponding author. Tel.: +91 941 536 4799.
E-mail address: akc1278@gmail.com (A. Kumar).

0272-8842/$ - see front matter © 2013 Elsevier Ltd and Techna Group S.r.l. All rights reserved.
http://dx.doi.org/10.1016/j.ceramint.2013.07.080

particle size variation of SiC on the electromagnetic and microwave absorption properties [16–20].

Nowadays, microwave absorber with broad absorption characteristics and less weight is required. It is observed from the literature that composite materials show better microwave absorption characteristics than single material. Such broadband characteristic could be achieved by combining different types of microwave absorber. Therefore, there is a need to improve absorption characteristics by tailoring the available materials to from new composite materials. Many composites combining dissimilar material like CB/SiC [21], soft/hard ferrite, CNT/ferrite [22], OLC/PMMA [23], coating of particles [24] etc. have been studied. Many researchers have tried to disperse metal particles to improve mechanical properties [25–27], however, little reported work is available regarding the use of metal dispersion in SiC as microwave absorber. The microwave absorption enhances due to the increased number of interaction with the dispersed metal particles [28]. Composites having too large metal particles present too small value of permeability due to strong eddy current loss and weak resonance [29,30]. For microwave absorbing characteristics, the metal particles should be smaller than the skin-depth for suppressing the eddy current phenomenon and these smaller particles should be uniformly dispersed in the dielectric medium to avoid agglomeration [31].

Therefore, in this paper an attempt has been made to see the effect of particle size of SiC powder and the effect of different metal particles dispersion in SiC on electromagnetic and microwave absorption properties in the frequency range of 8.2–12.4 GHz. The as-received SiC powder was reduced in size from micron- to nanosize by means of milling and the corresponding effect of particle size variation on electromagnetic and microwave absorption properties was studied. In order to see the effect of metal particle dispersion on microwave absorption, different metal powders were dispersed in SiC by means of milling and simultaneously the metal particles are reduced in size to avoid the skin depth phenomenon. In this paper, Section 2 briefly describes about the experimental setup and procedure for the reduction in particle size of SiC powder and the dispersion of metal particles. It also discusses about the characterization techniques used in this study. The results of characterizations are discussed in Section 3, which is followed by conclusion in Section 4.

2. Experimental setup and procedure

The SiC powder (Sigma-Aldrich, purity $>98\%$, 200–450 mesh) was used as the starting material in the present study. The as-received SiC powder was first passed through sieves of 325 and 400 meshes; and then the powder was milled in a high energy planetary ball mill (Model: Retsch, PM 400/2, Germany) at 300 rpm for different periods of time (1, 2, 3, 6, 10 and 20 h). Hardened steel balls of diameters 18, 8 and 4 mm were used for milling the powder in a cylindrical stainless steel jar in toluene medium. The ball to powder weight ratio (BPR) was 10:1. After milling, the milled powder was dried at 40 °C in vacuum oven till it dried completely. The milling resulted in a significant reduction of the particle size with increasing milling time. To see the effect of metal-dispersion on the electromagnetic and microwave absorption characteristic, 10 wt% of metal powder was dispersed in SiC powder through milling. Different magnetic and non-magnetic elements like Al, Co, Cr, Mn, Ni, Ti and Zn (size: 325 meshes) were dispersed in SiC powder and milled for 10 h at 300 rpm. The details of different milled samples with and without metal dispersion are listed in Tables 1 and 2.

The phases present in the milled powder samples were determined by an X-ray diffractometer (Bruker's AXS D8 Advance) using Cu-Kα radiation (λ=1.5406 Å). The crystallite size of the milled samples was calculated from the full width at half maximum (FWHM) corresponding to the highest diffracted peak by applying Suryanarayana and Grant Norton's formula [32,33]. The morphologies of the milled powder samples were analyzed by a field emission-scanning electron microscope (QUANTA FEG 200 FEI). The quantitative metallographic approach was used to determine average particle size and standard deviation of the milled SiC powder samples using a FE-SEM micrograph and confirmed by the Zeta particle size analyzer (Malvern Zetasizer ZS90). To study the complex dielectric properties, SiC-epoxy composites were prepared by homogeneously mixing the milled powder with 20 wt% epoxy and pressing into rectangular pellet of 2.2 mm thickness. These epoxy compacts were cured at 60 °C for 2 h. The prepared compacts were machined and polished to exactly fit into the measuring waveguide (WR-90). The scattering parameters (S_{11} and S_{21}) were measured using a Vector Network Analyzer (Agilent N5222 PNA series). These parameters were then used to determine relative complex permittivity ($\varepsilon_r=\varepsilon'-\varepsilon''$) and permeability ($\mu_r=\mu'-\mu''$) values using a 'Poly Ref/Tran μ & ε Polynomial Fit' model of Agilent materials measurement software 85071 in the frequency range of 8.2–12.4 GHz at room temperature. The values of reflection loss (RL) were calculated from the relative complex permittivity (ε_r) and permeability (μ_r) at given frequency (f) and absorber thickness (d) with the following equations:

$$Z_{in} = Z_o\left(\mu_r/\varepsilon_r\right)^{1/2}\tanh\left\{j\left(2\pi f d/c\right)\left(\mu_r\varepsilon_r\right)^{1/2}\right\}$$

$$RL = -20\log\left|\left(Z_{in}-Z_o\right)/\left(Z_{in}+Z_o\right)\right|$$

where, Z_{in}–input impedance of absorber, Z_o–impedance of free space and c–velocity of light.

3. Results and discussion

3.1. Phase analysis

XRD analysis provides detailed information on crystallite structure characteristics. Fig. 1 shows the indexed XRD patterns of as-received as well as milled silicon carbide powder samples S_1–S_8. The XRD peaks of as-received SiC samples S_1 and S_2 correspond to β-silicon carbide (Moissanite 6H; ICSD Collection Code: 27051) with 2θ=34.083°, 35.644°, 38.123°, 59.926°, 59.983°, 65.616°, 71.740° and 71.765°, attributed to

Table 1
Details of XRD analysis, particles size and microwave absorption properties of milled SiC samples.

Code	Milling time (h)	Avg. particle size ± Std. Dev.	Crystallite size (nm)	Lattice parameters (Å)		I_{Fe}/I_{max}	Frequency max RL (GHz)	Thickness max RL (mm)	Max RL (dB)	Absorption bandwidth < -10 dB (GHz)
				a	c					
S_1(200–325)	0	66.7 ± 14.47 μm	84.4	3.084	15.114	0	10.888	2.0	−16.23	1.932
S_2(325–400)	0	35.2 ± 9.73 μm	84.4	3.084	15.114	0	10.636	2.0	−15.84	2.016
S_3	1	3.01 ± 2.30 μm	69.2	3.083	15.112	0.14	9.628	2.0	−23.70	2.184
S_4	2	1.00 ± 1.11 μm	67.5	3.082	15.101	0.24	9.796	1.9	−43.67	2.352
S_5	3	808 ± 831 nm	63.3	3.081	15.101	0.30	9.460	1.9	−50.71	2.520
S_6	6	461 ± 408 nm	53.5	3.083	15.232	0.43	10.216	1.7	−16.67	2.856
S_7	10	176 ± 201 nm	47.2	3.084	15.291	0.56	10.300	1.6	−15.94	2.856
S_8	20	71 ± 34 nm	35.8	3.082	14.767	0.75	10.552	1.8	−27.17	2.688

Table 2
Details of XRD analysis and microwave absorption properties of metal dispersed SiC based composites, milled for 10 h at 300 rpm.

Code	Sample	2θ values for 2nd phase (deg)	$2\theta_{Fe}$ (deg)	ICSD code for 2nd phase	I_{Fe}/I_{max}	Frequency max RL (GHz)	Thickness max RL (mm)	Max RL (dB)	Absorption bandwidth < -10 dB (GHz)	Min skin depth (nm)
M_1(S_7)	SiC	35.560[a]	44.583	27051[b]	0.56	10.300	1.6	−15.94	2.856	20
M_2	SiC+Al	38.575	44.653	53775	0.08	8.284	2.2	−19.58	1.008	759
M_3	SiC +Co	44.183	44.681	76632	0.16	11.560	1.8	−24.31	2.604	71
M_4	SiC+Cr	44.363	44.645	625715	0.27	10.888	1.7	−37.08	3.024	2000
M_5	SiC +Mn	42.964	44.573	642935	0.19	10.300	1.8	−43.35	3.024	614
M_6	SiC+Ni	44.336	44.672	76667	0.25	11.812	1.5	−24.93	2.100	49
M_7	SiC+Ti	40.094	44.672	76144	0.10	8.704	2.1	−40.16	1.848	2928
M_8	SiC +Zn	43.102	44.430	53769	0.11	9.376	2.0	−43.69	2.604	3470

[a] 2θ value corresponding to highest peak of SiC.
[b] ICSD Collection Code for SiC.

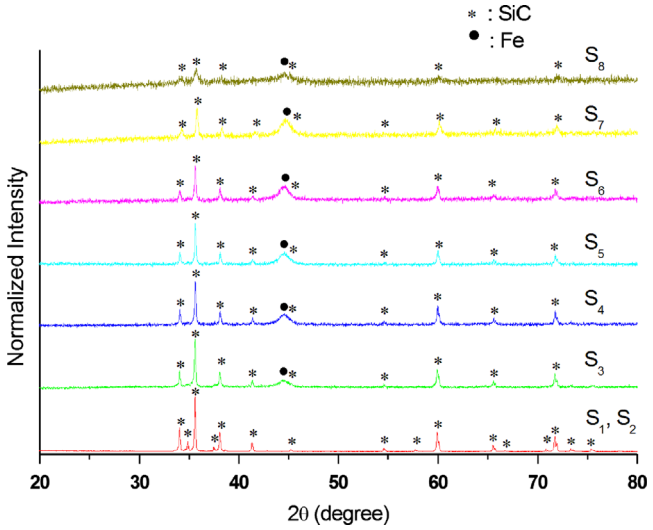

Fig. 1. XRD patterns of the milled SiC powder for various milling durations (samples S_1–S_8).

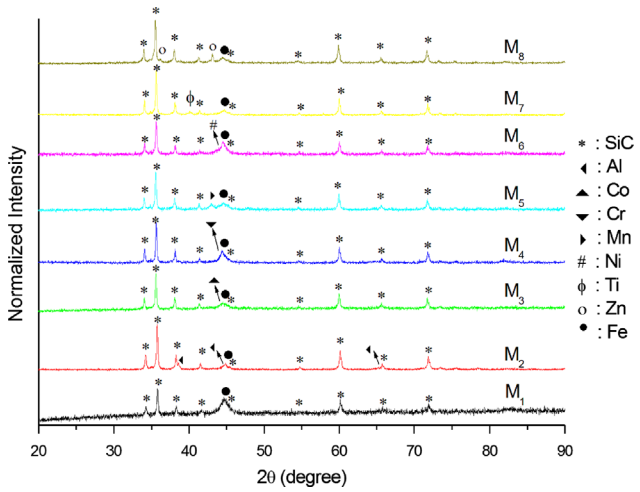

Fig. 2. XRD patterns of the milled metal dispersed SiC composites (samples M_1–M_8) for 10 h.

(011), (012), (013), (018), (110), (019), (116) and (022) planes respectively. With milling iron pickup from the steel balls starts, which is identified as α-Fe ($2\theta = 44.663^\circ$, ICSD Collection Code for Fe: 631729) and the relative integrated intensity of α-Fe peak increases from sample S_3 to S_8 indicating that the rate of iron pickup increases with milling time (Table 1). Simultaneously, with the increase in milling time, the relative integrated intensities of the peaks corresponding to SiC decreased. It is also observed from the XRD patterns of the milled SiC samples that the amorphization in samples increases with milling from samples S_3 to S_8, which can be explained by the accumulation of dislocations leading to changes in stacking sequences during milling [34]. As prolonged milling cause more dislocations, the cascading motion of the partial planes on neighboring planes may cause the accumulation of the defects and thereby increases the system energy tremendously to cause amorphous structure [35]. This amorphization can also be understood as the values of lattice parameters change with milling time (Table 1) and this distortion in lattice parameters is due to severe plastic deformation during milling. The values of lattice parameters start reducing with the increase in the milling time up to sample S_5 but thereafter the increase in lattice parameters is due to stretching in the lattices as more and more iron particles enter into the SiC crystal structure. However, with further milling these values again decrease due to further reduction in particle size because of continuous impaction. The crystallite size of the SiC particles reduces with milling time (Table 1). The as-received SiC powder with average particle size of 66.7 μm reduces to 176 nm (average size) in 10 h of milling. Thereafter rate of reduction in average particle size is very slow i.e., SiC powder reduces from an average particle size of 176 nm to 71 nm in the next 10 h of milling which consume energy. Therefore, 10 h milling time has been selected to have a balance between particle size and amorphization for further dispersion of different metal particles. The XRD patterns of milled SiC powders after metal dispersion are shown in Fig. 2. With the dispersion of metal particles, extra peaks corresponding to dispersed metals have been found in the samples M_2–M_8 and the summary of XRD analysis is listed in Table 2. The intensity of the peaks corresponding to the dispersed metals is found to be smaller as only 10 wt% metals were dispersed in SiC powder. As the dispersed metals are ductile and less hard than SiC, they form a protective layer on the surface of the balls which restrains steel balls from adhesive wear and the amount of iron pickup reduces. Therefore, the integrated intensity of the peak corresponding to iron ($2\theta = 44.663^\circ$) decreases (Fig. 2).

3.2. Morphological analysis

The morphologies of all the samples with and without metal dispersion have been investigated by FE-SEM. The morphological change that has taken place before and after milling of the SiC powder samples without metal dispersion is shown in Fig. 3. The average particle size and standard deviation of the milled powder samples, without metal dispersion are listed in Table 1. The as-received SiC powder after sieving is shown as S_1 and S_2 with the average particle size of 66.7 and 35.2 μm respectively. With the increase in milling time, the particles break down into smaller particles. According to Table 1, the average particle size and the standard deviation both reduce with milling time because the bigger particles undergo larger extent of impact and shear, and reduce more easily. The irregular shaped particles become more regular after milling. After 10 h of milling, the average particle size reduces to 176 nm and the particles are less regular in shape containing some sharp edges, however, after 20 h of milling particles reduce to less than 71 nm (average size) and are more regular in shape.

Fig. 4 shows the FE-SEM micrographs of different metal dispersed SiC powders milled for 10 h. The sharp cleaved surfaces marked as region 'A' in sample M_1 (S_7) reveal that the particles break into smaller size particles because of the brittle nature of SiC. The morphology of the metal-dispersed

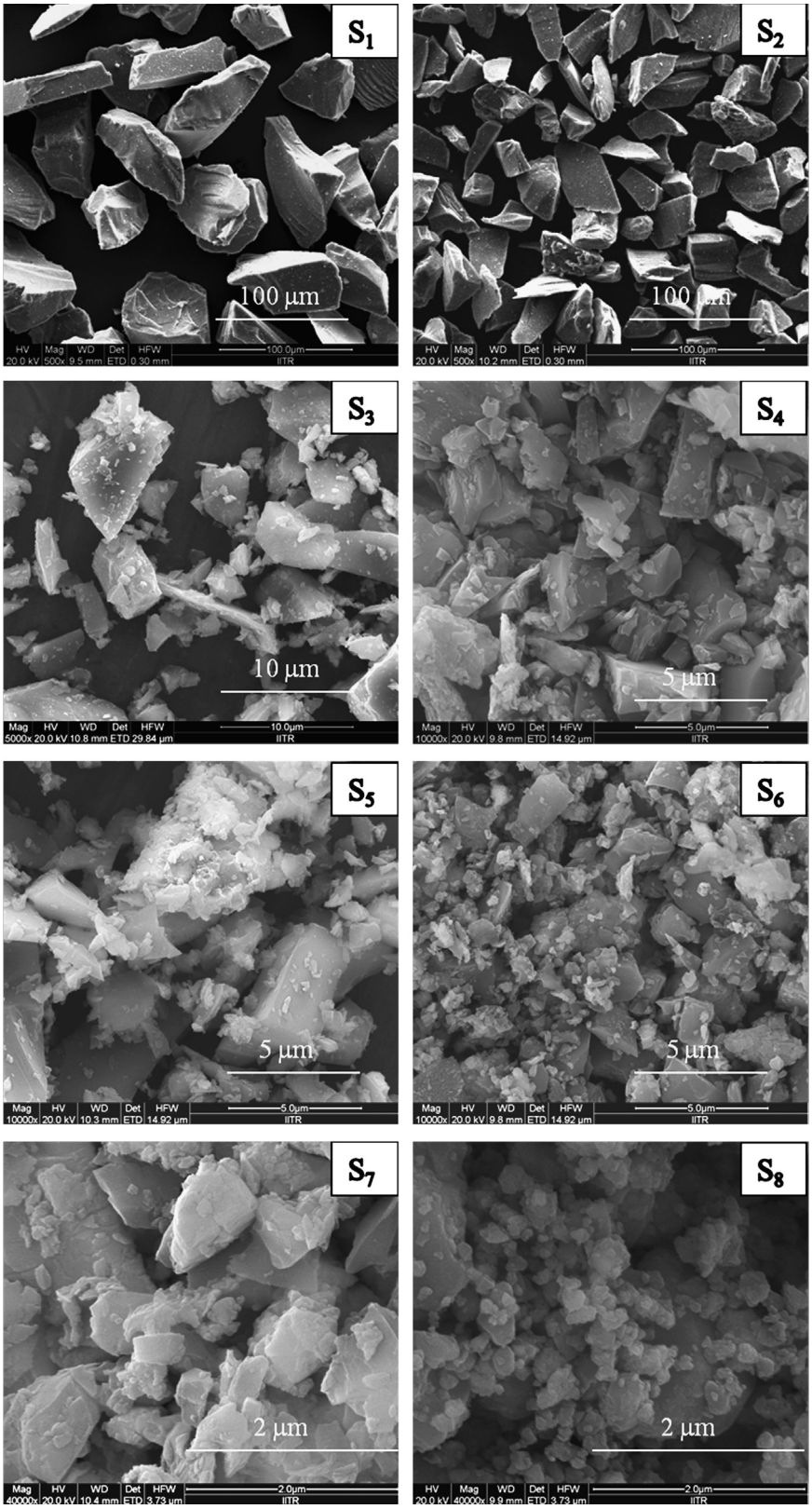

Fig. 3. FE-SEM micrographs of the milled SiC powder samples S_1–S_8.

SiC powders change with the hardness of the dispersed metal, as the relative hardnesses of the different metallic particles are different. With the dispersion of the softer metals like Al and Zn, the particles are getting elongated and are forged onto one another making layered structures (marked as region 'B') as seen more predominantly in the samples M_2 and M_8. On the

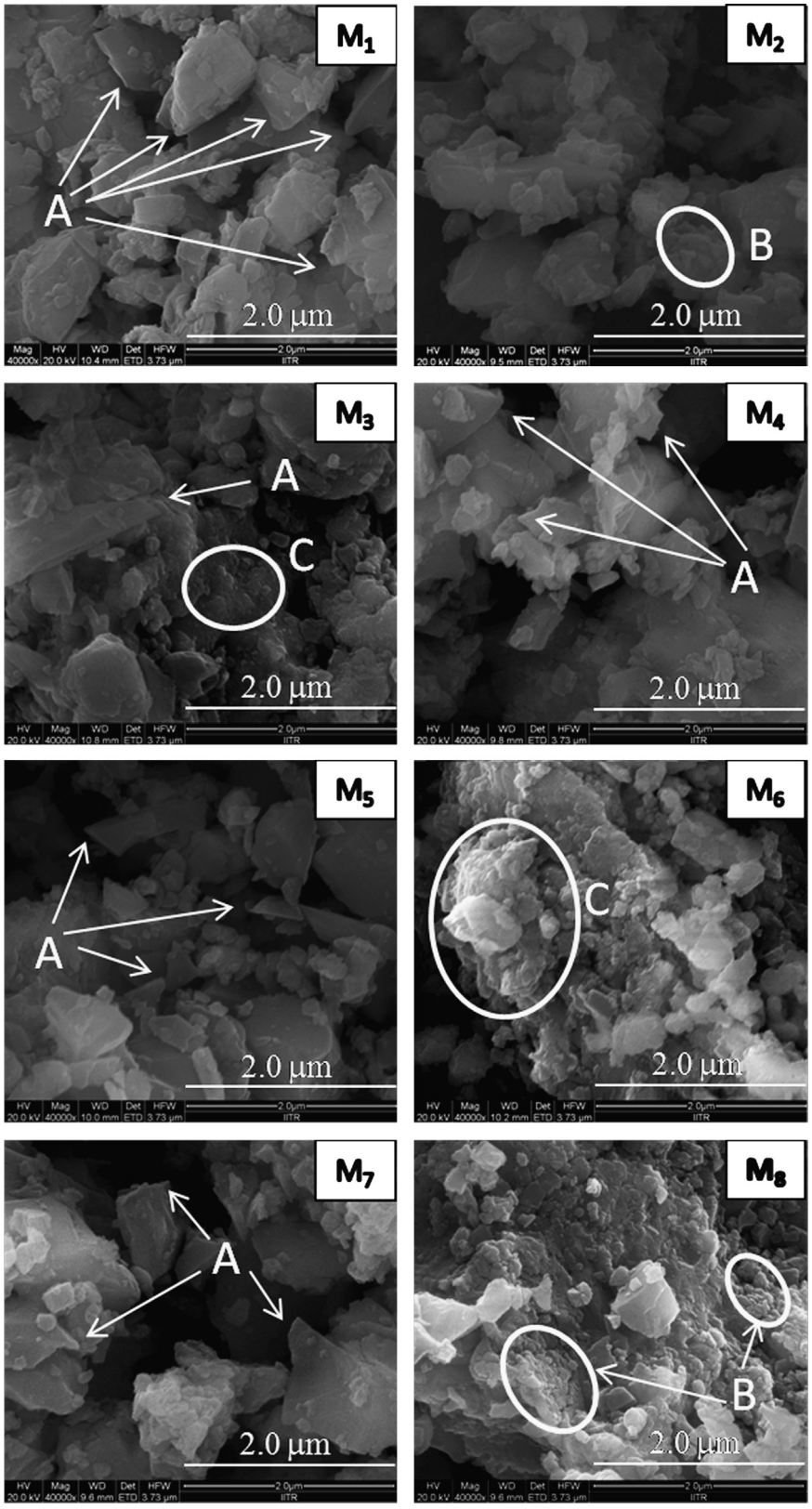

Fig. 4. FE-SEM micrographs of the milled metal dispersed SiC composite samples M_1–M_8.

other hand, with the dispersion of the harder elements like Cr, Mn and Ti, the particles are getting reduced in size and seem to disperse in SiC matrix with cleaved brittle surfaces marked as region 'A' in the micrographs for the samples M_4, M_5 and M_7, however, the number of the cleaved surfaces is less in comparison to sample M_1. With the dispersion of Co and Ni

metals, particles get reduced to spherical shape and seen to be agglomerated because of the ferromagnetic nature of the elements, Ni and Co, as marked in region 'C' in the samples M_3 and M_6 respectively.

3.3. Dielectric constant measurement

The dielectric constant values of the milled SiC powder-epoxy composite as a function of frequency at *X*-band are shown in Fig. 5. The real parts (ε', μ') of complex permittivity and permeability represent the storage capability of electric and magnetic energy. The imaginary parts (ε'', μ'') represent the loss of electric and magnetic energy [18]. Fig. 5a shows that the ε' decreases with the increase in frequency however, the ε'' nearly remains constant with frequency. Both the ε' and ε'' values increase with the decrease in particle size from sample S_1 to S_7, however, for sample S_8 the ε' and ε'' values decrease as the content of iron pickup increases tremendously in the milled sample S_8 as observed from XRD analysis (Fig. 1). As evident from Table 1, the particle size of SiC decreases from

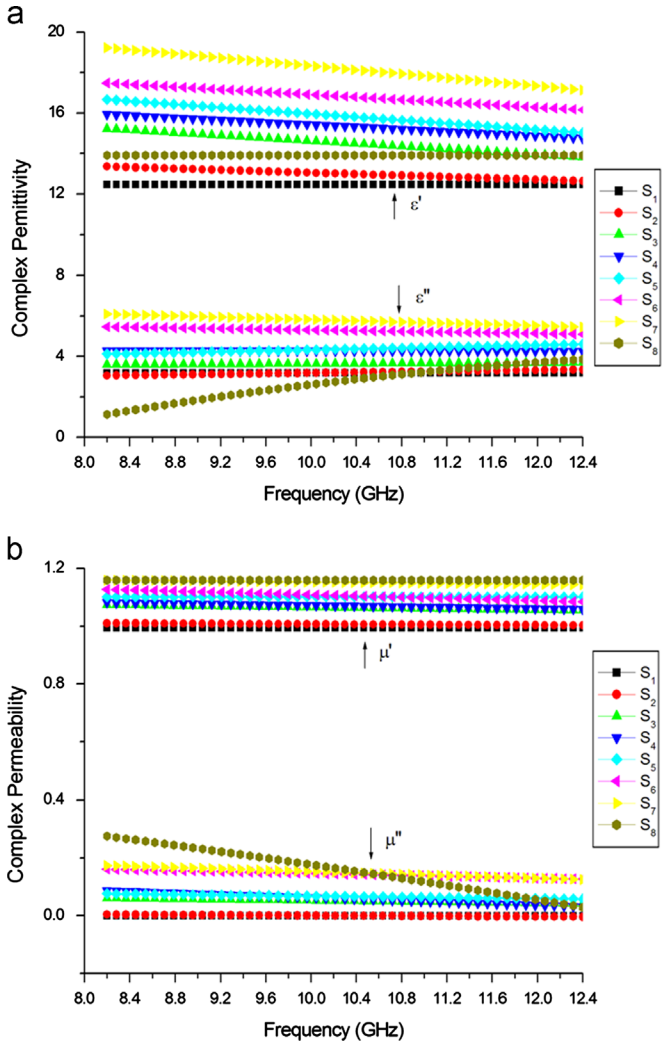

Fig. 5. Frequency dependence of (a) the real part ε' and imaginary part ε'' of complex permittivity and (b) the real part μ' and imaginary part μ'' complex permeability of the milled SiC-epoxy composite samples S_1–S_8.

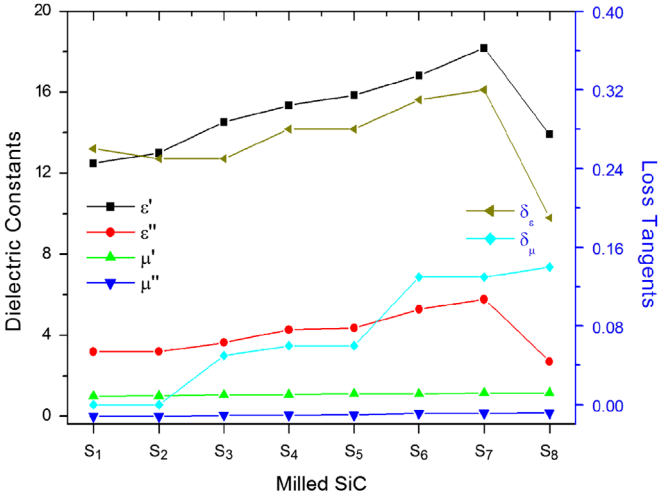

Fig. 6. Average complex dielectric properties with of the milled SiC-epoxy composite samples S_1–S_8 with milling time.

sample S_1 to S_7 and correspondingly surface area of the particles increases. With the increase in surface area space charge polarization becomes more dominant and as a result the complex permittivity increases [36]. The average value of ε' increases from 12.47 to 18.18 for samples S_1–S_7 and corresponding ε'' increases from an average value of 3.19–5.78. The average values of ε' and ε'' for sample S_8 are 13.91 and 2.70 respectively. The average value of μ' and μ'' increases in a small fraction with the decrease in particle size and is shown in Fig. 6. SiC being a non-magnetic material has permeability $\mu'=1$ and $\mu''=0$, however, due to the dilution effect induced by milling with hardened steel balls, iron pickup took place and complex permeability values increase. Fig. 6 shows that the magnetic loss tangent (δ_μ) values are smaller (less than 0.06) up to sample S_5 (i.e., up to 3 h of milling), however, δ_μ value increases to more than 0.13 due to increase in iron content with further milling.

Fig. 7 represents the real part (ε') and imaginary part (ε'') of permittivity for metal dispersed SiC powder-epoxy composites as a function of frequency at *X*-band. The space charge polarization plays an important role in metal dispersed ceramics. The free electrons from the metallic particles increase the charge at the metal dielectric interface and allows the space charge polarization to take place. Therefore, the permittivity of the composite improves due to improved conductivity as compared with samples S_1 and S_2 [37]. It is observed from Fig. 7a that the values of ε' and ε'' decrease with the increase in frequency. The value of the ε' for sample M_1 is observed to be more in comparison to metal dispersed SiC epoxy composite as the fraction of picked-up iron in sample M_1 is more in comparison to other samples M_2–M_8 (Table 2). The values of the real part (μ') and imaginary part (μ'') of complex permeability for metal dispersed SiC are shown in Fig. 7b. The μ' remains nearly constant with the increase in frequency however, the values of the μ'' vary with metal dispersion as magnetic properties are different for dispersed-metals. Fig. 8 shows the change in the average values of complex permittivity and permeability with metal dispersion in SiC. It is observed that the dielectric constant

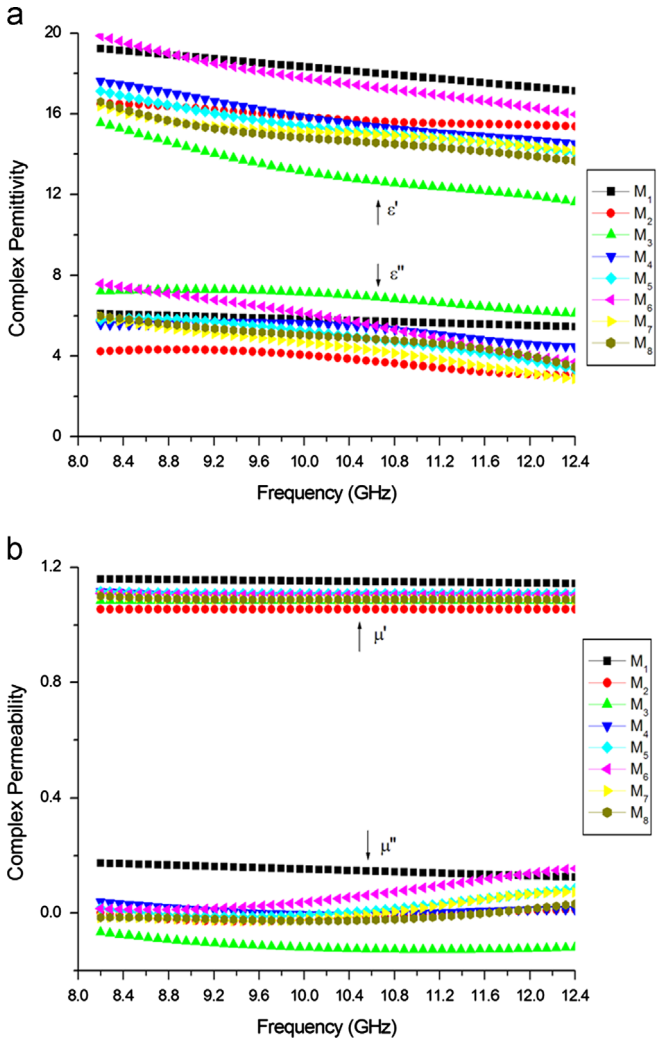

Fig. 7. Frequency dependence of (a) the real part ε' and imaginary part ε'' of complex permittivity and (b) the real part μ' and imaginary part μ'' complex permeability of the metal dispersed SiC-epoxy composite samples M_1–M_8.

value moves around the average line except in the case of Ni and Co dispersion because of their ferromagnetic character. In case of sample M_1 the dielectric constant values are higher as the iron content in the sample M_1 is high in comparison to metal-dispersed SiC samples (Table 2).

3.4. Reflection loss study

Fig. 9 shows the effect of particle size on the calculated reflection loss (RL) for milled SiC powder-epoxy composites and the detailed data for RL are summarized in Table 1. It is observed from RL results that with the reduction in particle size, the maximum values of RL first increased with the milling time up to 3 h (i.e., up to sample S_5) and then decreased to 10 h of milling (i.e., for sample S_7). This decrease in the values of RL in the samples S_6 and S_7 may be due to the fact that iron enters into the crystal structure of SiC, leaving no vacancy in the crystal structure. This variation in reflection loss indicates that magnetic properties start dominating over dielectric properties after certain milling time. The loss tangent is defined as the ratio of the imaginary part to the real part and represents the loss of EM energy. The variation in the RL values can be explained on the basis of dielectric loss tangent. With the decrease in particle size, the dielectric loss tangent (δ_ε) increases and therefore RL value increases, however, with further milling the iron pickup took place and therefore bandwidth increases with the decrease in maximum RL values. With prolonged milling (for sample S_8) the δ_ε decreases to a much lower value (0.19) and δ_μ increases resulting in an increase in the RL values. For sample S_8, the values of RL are higher due to high iron pickup in this sample. It is observed that the matching thickness, which describes the thickness of maximum RL, decreases with decrease in particle size of SiC (Table 1) as well as the effective absorption bandwidth corresponding to −10 dB level increases from 1.932 GHz to

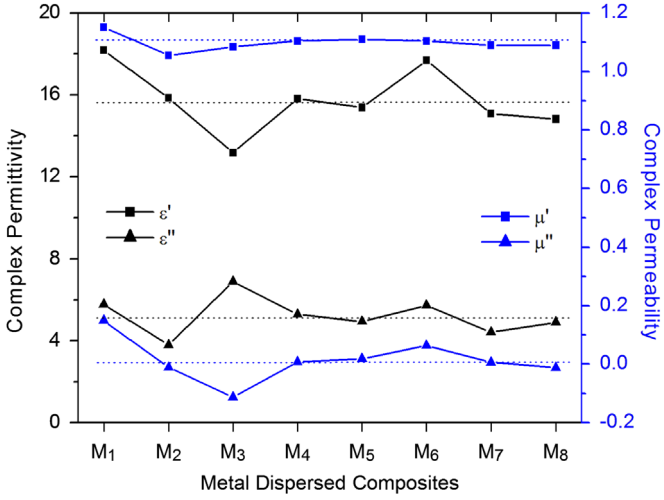

Fig. 8. Effect of metal-dispersions in SiC-epoxy composite on the average complex dielectric properties.

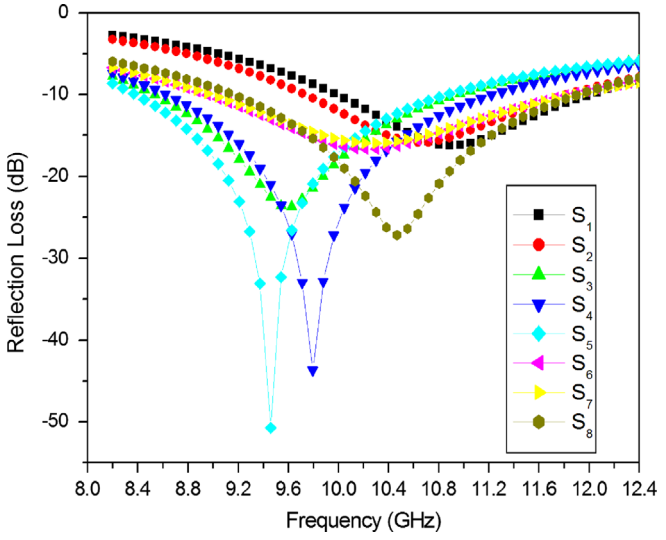

Fig. 9. Frequency dependent RL for the milled SiC-epoxy composite samples S_1–S_8.

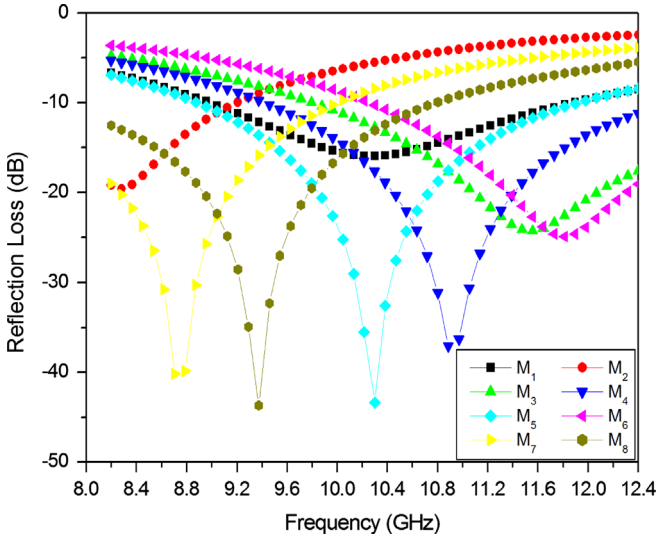

Fig. 10. Frequency dependent RL for the milled metal-dispersed SiC-epoxy composite samples M_1–M_8.

2.856 GHz with the decrease in particle size from sample S_1 (66.7 ± 14.47 μm) to sample S_7 (176 ± 201 nm).

The RL characteristics of metal dispersed SiC powder-epoxy composites are shown in Fig. 10 and the detailed data for RL are summarized in Table 2. It is observed from RL data that the maximum values of RL increase with the dispersion of metal-particles in SiC. The maximum value of RL for sample M_1 is -15.94 dB at 10.3 GHz, which improves to a maximum value of -37.08 dB at 10.888 GHz and -43.35 dB at 10.3 GHz with a bandwidth of 3.024 GHz for dispersion of Cr and Mn metals respectively. The variation in the maximum value of reflection loss has shown some trend with skin depth. The amount of reflection loss is observed to be less in the case of Co and Ni metal dispersions in comparison to other metal dispersion in SiC except Al metal, as the value of skin depth is less for Co and Ni metals (Table 2). This improvement in microwave absorption due to metal-dispersion could be understood as the EM wave is incident on a metal-dispersed ceramic, it goes through multiple internal reflections within the material before coming out of the material and as a result the EM waves travel longer and attenuate as a series of interactions with the metal particles [4].

4. Conclusion

The 'as-received' SiC was reduced in smaller particle through ball milling and the effect of particle size of SiC on the complex dielectric and microwave absorption properties was studied in *X*-band. It is observed that complex dielectric and absorption properties enhance with the reduction in particle size of SiC. Moreover, the matching thickness decreases and absorption band (< -10 dB) is broadened. The metal particles of different metals are dispersed in SiC through the milling process. The metal dispersed SiC-epoxy composites show enhancement in EM absorption characteristic. The maximum RL was found to improve to -37.08 dB at 10.888 GHz for an absorber thickness of 1.7 mm for Cr dispersed SiC and -43.35 dB at 10.300 GHz for an absorber thickness of 1.8 mm for Mn dispersed SiC. It can be concluded that, with the metal dispersion in small quantity in dielectric matrix, maximum RL and bandwidth corresponding to -10 dB level increases.

References

[1] K.J. Vinoy, R.M. Jha, Trends in radar absorbing materials technology, Sadhana 20 (1995) 815–850.
[2] X.G. Liu, B. Li, D.Y. Geng, W.B. Cui, F. Yang, Z.G. Xie, D.J. Kang, Z.D. Zhang, Fe, Ni/C nanocapsules for electromagnetic-wave-absorber in the whole Ku-band, Carbon 47 (2009) 470–474.
[3] A.N. Yusoff, M.H. Abdullah, S.H. Ahmad, S.F. Jusoh, A.A. Mansor, S.A.A. Hamid, Electromagnetic and absorption properties of some microwave absorbers, Journal of Applied Physics 92 (2002) 876–882.
[4] F. Qin, C. Brosseau, A review and analysis of microwave absorption in polymer composites filled with carbonaceous particles, Journal of Applied Physics 111 (2012) 1–24.
[5] B. Zhang, J. Li, J. Sun, S. Zhang, H. Zhai, Z. Du, Nanometer silicon carbide powder synthesis and its dielectric behavior in the GHz range, Journal of the European Ceramic Society 22 (2002) 93–99.
[6] S.V. Egorov, A.G. Eremeev, I.V. Plotnikov, K.I. Rybakov, V.V. Kholoptsev, Y.V. Bykov, Absorption of microwaves in metal–ceramic powder materials, Radiophysics and Quantum Electronics 53 (2010) 354–362.
[7] S.M. Wiederhorn, B.J. Hockey, J.D. French, Mechanisms of deformation of silicon nitride and silicon carbide at high temperatures, Journal of the European Ceramic Society 19 (1999) 2273–2284.
[8] S. Hayuna, V. Paris, R. Mitrani, S. Kalabukhov, M.P. Dariel, E. Zaretsky, N. Frage, Microstructure and mechanical properties of silicon carbide processed by Spark Plasma Sintering (SPS), Ceramics International 38 (2012) 6335–6340.
[9] H. Morkoc, S. Strite, G.B. Gao, M.E. Lin, B. Sverdlov, M. Burns, Large band gap SiC, III–V nitride, and II–VI ZnSe based semiconductor device technologies, Journal of Applied Physics 76 (1994) 363–1398.
[10] Z. Li, W. Zhou, T. Lei, F. Luo, Y. Huang, Q. Cao, Microwave dielectric properties of SiC(B) solid solution powder prepared by sol–gel, Journal of Alloys and Compounds 475 (2009) 506–509.
[11] Z. Li, H. Du, X. Liu, F. Luo, W. Zhou, Synthesis and microwave dielectric properties of Si/C/B powder, Transactions of Nonferrous Metals Society of China 16 (2006) 470–473.
[12] G. Zou, M. Cao, H. Lin, H. Jin, Y. Kang, Y. Chen, Nickel layer deposition on SiC nanoparticles by simple electroless plating and its dielectric behaviors, Powder Technology 168 (2006) 84–88.
[13] F. Luo, H. Jiao, D. Zhu, W. Zhou, Dielectric properties of SiC/LAS composite, Materials Letters 59 (2005) 105–109.
[14] Z. Li, W. Zhou, X. Su, F. Luo, Y. Huang, C. Wang, Effect of boron doping on microwave dielectric properties of SiC powder synthesized by combustion synthesis, Journal of Alloys and Compounds 509 (2011) 973–976.
[15] J.G. Hartnett, D. Mouneyrac, J. Krupka, J.M. Floch, M.E. Tobar, D. Cros, Microwave properties of semi-insulating silicon carbide between 10 and 40 GHz and at cryogenic temperatures, Journal of Applied Physics 109 (2011) 1–4.
[16] S. Rajesh, K.P. Murali, V. Priyadarsini, S.N. Potty, R. Ratheesh, Rutile filled PTFE composites for flexible microwave substrate applications, Materials Science and Engineering: B 163 (2009) 1–7.
[17] R. Laiho, E. Lahderanta, Y.P. Stepanov, L.S. Vlasenko, Microwave absorption in micron- and nano-size YBaCuO powders, Physica B 284–288 (2000) 947–948.
[18] K.P. Murali, S. Rajesh, K.J. Nijesh, R. Ratheesh, Effect of particle size on the microwave dielectric properties of alumina-filled PTFE substrates, International Journal of Applied Ceramic Technology 7 (2010) 475–481.
[19] L. Liu, Y. Duan, J. Guo, L. Chen, S. Liu, Influence of particle size on the electromagnetic and microwave absorption properties of FeSi/paraffin composites, Physica B 406 (2011) 2261–2265.

[20] A. Kumar, V. Agarwala, D. Singh, Effect of particle size of $BaFe_{12}O_{19}$ on the microwave absorption characteristics in X-band, Progress in Electromagnetics Research M 29 (2013) 223–236.
[21] X. Liu, Z. Zhang, Y. Wu, Absorption properties of carbon black/silicon carbide microwave absorbers, Composites: Part B 42 (2011) 326–329.
[22] S. Tyagi, P. Verma, H.B. Baskey, R.C. Agarwala, V. Agarwala, T.C. Shami, Microwave absorption study of carbon nano tubes dispersed hard/soft ferrite nanocomposite, Ceramics International 38 (2012) 4561–4571.
[23] S.A. Maksimenko, V.N. Rodionova, G.Y. Slepyan, V.A. Karpovich, O. Shenderova, J. Walsh, V.L. Kuznetsov, I.N. Mazov, S.I. Moseenkov, A.V. Okotrub, P. Lambin, Attenuation of electromagnetic waves in onion-like carbon composites, Diamond and Related Materials 16 (2007) 1231–1235.
[24] R. Sharma, R.C. Agarwala, V. Agarwala, Development of electroless (Ni–P)/$BaNi_{0.4}Ti_{0.4}Fe_{11.2}O_{19}$ nanocomposite powder for enhanced microwave absorption, Journal of Alloys and Compounds 467 (2009) 357–365.
[25] H. Sakasegawa, M. Tamura, S. Ohtsuka, S. Ukai, H. Tanigawa, A. Kohyama, M. Fujiwara, Precipitation behavior of oxide particles in mechanically alloyed powder of oxide-dispersion-strengthened steel, Journal of Alloys and Compounds 452 (2008) 2–6.
[26] E.A. Levashov, P.V. Vakaev, E.I. Zamulaeva, A.E. Kudryashov, V.V. Kurbatkina, D.V. Shtansky, A.A. Voevodin, A. Sanz, Disperse-strengthening by nanoparticles advanced tribological coatings and electrode materials for their deposition, Surface and Coatings Technology 201 (2007) 6176–6181.
[27] L. Geng, H.W. Zhang, H.Z. Li, L.N. Guan, H.U. Lujun, Effects of Mg content on microstructure and mechanical properties of SiCp/Al–Mg composites fabricated by semi-solid stirring technique, Transactions of Nonferrous Metals Society of China 20 (2010) 1851–1855.
[28] L.G. Grechko, V.N. Pustovit, K.W. Whites, Dielectric function of aggregates of small metallic particles embedded in host insulating matrix, Applied Physics Letters 76 (2000) 1854–1856.
[29] S.S. Kim, S.T. Kim, Y.C. Yoon, K.S. Lee, Magnetic, dielectric, and microwave absorbing properties of iron particles dispersed in rubber matrix in gigahertz frequencies, Journal of Applied Physics 97 (2005)1–3.
[30] P. Toneguzzo, G. Viau, O. Acher, F.F. Vincent, F. Fievet, Monodisperse ferromagnetic particles for microwave applications, Advanced Materials 10 (1998) 1032–1035.
[31] Z. Xie, D. Geng, X. Liu, S. Ma, Z. Zhang, Magnetic and microwave-absorption properties of graphite-coated (Fe, Ni) nanocapsules, Journal of Materials Science and Technology 27 (2011) 607–614.
[32] I.J. Shon, I.Y. Ko, S.H. Jo, J.M. Doh, J.K. Yoon, S.W. Park, Mechanochemical synthesis and rapid consolidation of nanocrystalline 3NiAl–Al_2O_3 composites, Journal of Nanomaterials (2011) (Article ID 793135), doi:10.1155/2011/793135.
[33] I.J. Shon, H.J. Wang, S.W. Cho, W. Kim, Mechanical synthesis and rapid consolidation of nanocrystalline TiAl–Al_2O_3 composites by high frequency induction heated sintering, Materials Transactions 52 (2011) 1832–1835.
[34] A.W. Weeber, H. Bakker, Amorphization by ball milling: a review, Physica B 153 (1988) 93–135.
[35] X.Y. Yang, Y.K. Wu, H.Q. Ye, Localized amorphization in SiC induced by ball milling, Journal of Materials Science Letters 20 (2001) 1517–1518.
[36] L. Liu, Y. Duan, J. Guo, L. Chen, S. Liu, Influence of particle size on the electromagnetic and microwave absorption properties of FeSi/paraffin composites, Physica B 406 (2011) 2261–2265.
[37] B. Lu, X.L. Dong, H. Huang, X.F. Zhang, X.G. Zhu, J.P. Lei, J.P. Sun, Microwave absorption properties of the core/shell-type iron and nickel nanoparticles, Journal of Magnetism and Magnetic Materials 320 (2008) 1106–1111.